

# Decay-lepton angular asymmetries in polarized $e^+e^- \rightarrow t\bar{t}$ as a measure of $CP$ -violating dipole couplings of the top quark

Saurabh D. Rindani<sup>1</sup>

*Theory Group, Physical Research Laboratory  
Navrangpura, Ahmedabad 380009, India*

## Abstract

In the presence of an electric dipole coupling of  $t\bar{t}$  to a photon, and an analogous “weak” dipole coupling to the  $Z$ ,  $CP$  violation in the process  $e^+e^- \rightarrow t\bar{t}$  leads to the polarization of the top and anti-top. This polarization can be analyzed by studying the angular distributions of decay charged leptons when the top or anti-top decays leptonically. We have obtained analytic expressions for these distributions when either  $t$  or  $\bar{t}$  decays leptonically, including  $\mathcal{O}(\alpha_s)$  QCD corrections in the soft-gluon approximation. The angular distributions are insensitive to anomalous interactions in top decay. We study two types of simple  $CP$ -violating polar-angle asymmetries and two azimuthal asymmetries which do not need the full reconstruction of the  $t$  or  $\bar{t}$ . We have evaluated independent 90% CL limits that may be obtained on the real and imaginary parts of the electric and weak dipole couplings at a linear collider operating at  $\sqrt{s} = 500$  GeV with integrated luminosity  $200 \text{ fb}^{-1}$  and also at  $\sqrt{s} = 1000$  GeV with integrated luminosity  $1000 \text{ fb}^{-1}$ . The effect of longitudinal beam polarization has been included.

## 1 Introduction

An  $e^+e^-$  linear collider operating at centre-of-mass (cm) energy of 500 GeV or higher and with an integrated luminosity of several hundred inverse femtobarns should be able to study with precision various properties of the top quark.

---

<sup>1</sup>Email address: saurabh@prl.ernet.in

While the standard model (SM) predicts  $CP$  violation outside the  $K$ -,  $D$ - and  $B$ -meson systems to be unobservably small, in some extensions of SM,  $CP$  violation might be considerably enhanced, especially in the presence of a heavy top quark. In particular,  $CP$ -violating electric dipole form factor of the top quark, and the analogous  $CP$ -violating “weak” dipole form factor in the  $t\bar{t}$  coupling to  $Z$ , could be enhanced. These  $CP$ -violating form factors could be determined in a model-independent way at high energy  $e^+e^-$  linear colliders, where  $e^+e^- \rightarrow t\bar{t}$  would proceed through virtual  $\gamma$  and  $Z$  exchange.

Since a heavy top quark with a mass of the order of 175 GeV decays before it hadronizes [1], it has been suggested [2] that top polarization asymmetry in  $e^+e^- \rightarrow t\bar{t}$  can be used to determine the  $CP$ -violating dipole form factors, since polarization information would be retained in the decay product distribution. There have been several proposals in which the  $CP$ -violating dipole couplings could be measured in decay momentum correlations or asymmetries with or without beam polarization. For a review see [3].

In this context it is important to note that top polarization can only be studied using top decay. However, for the information from decay distributions to reflect correctly top polarization, the decay amplitudes for various top polarization states have to be known accurately. In particular, if there are any anomalous effects in the decay process, they have to be known accurately. Alternatively, the decay distributions chosen for the study have to be insensitive to anomalous effects in the decay process. The single-lepton angular distributions that we discuss in this work satisfy the latter condition – they accurately reflect the polarization of the top quark resulting from the production process, while one can continue to use SM in the decay process.

In this paper we update some suggestions made [4, 5, 6] for the measurement of top dipole moments in  $e^+e^- \rightarrow t\bar{t}$  using angular asymmetries of the charged lepton produced in the semi-leptonic decay of one of  $t$  and  $\bar{t}$ , while the other decays hadronically. The improvements included in the update are several. Firstly, there is now a better idea of luminosities possible at a future linear collider like the proposed JLC. Together with updated values of beam polarization now considered feasible, the estimates of possible limits on dipole moments would be more realistic. Secondly,  $\mathcal{O}(\alpha_s)$  QCD corrections in the soft-gluon approximation have been now included. Thirdly, an assumption made in earlier work [4, 5, 6], that  $CP$  violation in top decay could be neglected, has been re-examined in light of recent work [7, 8]. It turns out that for angular asymmetries of the charged lepton considered here,  $CP$  violation in the decay (or for that matter even arbitrary  $CP$ -

conserving modifications of the  $tbW$  vertex) has no effect, if the  $b$ -quark mass is neglected. Thus the estimates in earlier work have been improved and put on sounder theoretical footing.

Earlier proposals have considered a variety of CP-violating observables, with varying sensitivities. These include, in addition to angular asymmetries, also vector and tensor correlations [9, 10], and expectation values of optimal variables [11]. (For a discussion on relative sensitivities of some variables, see [12]). We have chosen certain angular asymmetries here which have some advantages over others, even though they may not be the most sensitive ones. The advantages are: (i) Our asymmetries are in the laboratory frame, making them directly observable. (ii) They depend on final state momenta, rather than on top polarization. Polarization is measured only indirectly through the decay distributions. We therefore concentrate only on actual decay-lepton distributions, which are the simplest to observe. (iii) The observables we choose either do not depend on precise determination of energy and momentum of top quarks, or, in case of azimuthal asymmetries of the lepton, depend minimally on the top momentum direction for the sake of defining the coordinate axes. This has the advantage of higher accuracy. (iv) As stated before, leptonic angular distribution is free from background from CP violation in top decay, and gives a direct handle on anomalous couplings in top production. (v) The polar-angle asymmetries we consider can be obtained in analytical form, which is useful for making quick computations. It is possible to get analytical forms for certain azimuthal asymmetries as well, provided no angular cuts are imposed. (vi) The asymmetries considered here are rather simple conceptually, and hopefully, also from the practical measurement point of view.

Our single-lepton asymmetries have another obvious advantage, that since either  $t$  or  $\bar{t}$  is allowed to decay hadronically, there is a gain in statistics, as compared to double-lepton asymmetries.

Our results are based on fully analytical calculation of single lepton distributions in the production and subsequent decay of  $t\bar{t}$ . We present fully differential angular distribution as well as the distribution in the polar angle of the lepton with respect to the beam direction in the centre-of-mass (cm) frame for arbitrary longitudinal beam polarizations. These distributions for the standard model (SM) were first obtained by Arens and Sehgal [13]. Distributions including the effect of CP violation only in production were obtained in [5, 6], whereas, with all anomalous effects included in the  $\gamma t\bar{t}$  and  $Z t\bar{t}$  vertices, as well as decay  $tbW$  vertex were obtained in [7, 8]. Angular distributions in SM with  $\mathcal{O}(\alpha_s)$  QCD corrections in the soft-gluon approximation were obtained in [14]. The distributions including

anomalous effects in both top production and decay, and including  $\mathcal{O}(\alpha_s)$  QCD corrections in the soft-gluon approximation are presented here for the first time. While QCD corrections to  $e^+e^- \rightarrow t\bar{t}$  are substantial, to the extent of about 30% at  $\sqrt{s} = 500$  GeV, their effect on leptonic angular distributions is much smaller [14]. The main effect on the results will be to the sensitivity, through the  $1/\sqrt{N}$  factor, where  $N$  is the number of events.

The rest of the paper is organized as follows. In Sec. 2, we describe the calculation of the decay-lepton angular distribution from a decaying  $t$  or  $\bar{t}$  in  $e^+e^- \rightarrow t\bar{t}$ . In Sec. 3 we describe  $CP$ -violating asymmetries. Numerical results are presented in Sec. 4, and Sec. 5 contains our conclusions. The Appendix contains certain expressions which are too lengthy to be put in the main text.

## 2 Calculation of lepton angular distributions

We describe in this section the calculation of  $l^+$  ( $l^-$ ) distribution in  $e^+e^- \rightarrow t\bar{t}$  and the subsequent decay  $t \rightarrow bl^+\nu_l$  ( $\bar{t} \rightarrow \bar{b}l^-\bar{\nu}_l$ ). We adopt the narrow-width approximation for  $t$  and  $\bar{t}$ , as well as for  $W^\pm$  produced in  $t$ ,  $\bar{t}$  decay.

We assume the top quark couplings to  $\gamma$  and  $Z$  to be given by the vertex factor  $ie\Gamma_\mu^j$ , where

$$\Gamma_\mu^j = c_v^j \gamma_\mu + c_a^j \gamma_\mu \gamma_5 + \frac{c_d^j}{2m_t} i\gamma_5 (p_t - p_{\bar{t}})_\mu, \quad j = \gamma, Z, \quad (1)$$

with

$$\begin{aligned} c_v^\gamma &= \frac{2}{3}, \quad c_a^\gamma = 0, \\ c_v^Z &= \frac{\left(\frac{1}{4} - \frac{2}{3}x_w\right)}{\sqrt{x_w(1-x_w)}}, \\ c_a^Z &= -\frac{1}{4\sqrt{x_w(1-x_w)}}, \end{aligned} \quad (2)$$

and  $x_w = \sin^2\theta_w$ ,  $\theta_w$  being the weak mixing angle. In addition to the SM couplings  $c_{v,a}^{\gamma,Z}$  we have introduced the  $CP$ -violating electric and weak dipole form factors,  $ec_d^\gamma/m_t$  and  $ec_d^Z/m_t$ , which are assumed small. Use has also been made of the Dirac equation in rewriting the usual dipole coupling  $\sigma_{\mu\nu}(p_t + p_{\bar{t}})^\nu \gamma_5$  as

$i\gamma_5(p_t - p_{\bar{t}})_\mu$ , dropping small corrections to the vector and axial-vector couplings. We will work in the approximation in which we keep only linear terms in  $c_d^\gamma$  and  $c_d^Z$ . Addition of other  $CP$ -conserving form factors will not change our results in the linear approximation.

To include  $\mathcal{O}(\alpha_s)$  corrections in the soft-gluon approximation (SGA), we need to modify the above vertices, as explained in [14]. These modified vertices are given by

$$\Gamma_\mu^\gamma = c_v^\gamma \gamma_\mu + [c_M^\gamma + i\gamma_5 c_d^\gamma] \frac{(p_t - p_{\bar{t}})_\mu}{2m_t}, \quad (3)$$

$$\Gamma_\mu^Z = c_v^Z \gamma_\mu + c_a^Z \gamma_\mu \gamma_5 + [c_M^Z + i\gamma_5 c_d^Z] \frac{(p_t - p_{\bar{t}})_\mu}{2m_t}, \quad (4)$$

where

$$c_v^\gamma = \frac{2}{3}(1 + A), \quad (5)$$

$$c_v^Z = \frac{1}{\sin \theta_W \cos \theta_W} \left( \frac{1}{4} - \frac{2}{3} \sin^2 \theta_W \right) (1 + A), \quad (6)$$

$$c_a^\gamma = 0, \quad (7)$$

$$c_a^Z = \frac{1}{\sin \theta_W \cos \theta_W} \left( -\frac{1}{4} \right) (1 + A + 2B), \quad (8)$$

$$c_M^\gamma = \frac{2}{3}B, \quad (9)$$

$$c_M^Z = \frac{1}{\sin \theta_W \cos \theta_W} \left( \frac{1}{4} - \frac{2}{3} \sin^2 \theta_W \right) B. \quad (10)$$

The form factors  $A$  and  $B$  are given to order  $\alpha_s$  in SGA (see, for example, [15, 16] by

$$\begin{aligned} \text{Re}A = & \hat{\alpha}_s \left[ \left( \frac{1 + \beta^2}{\beta} \log \frac{1 + \beta}{1 - \beta} - 2 \right) \log \frac{4\omega_{\text{max}}^2}{m_t^2} - 4 \right. \\ & + \frac{2 + 3\beta^2}{\beta} \log \frac{1 + \beta}{1 - \beta} + \frac{1 + \beta^2}{\beta} \left\{ \log \frac{1 - \beta}{1 + \beta} \left( 3 \log \frac{2\beta}{1 + \beta} \right. \right. \\ & \left. \left. + \log \frac{2\beta}{1 - \beta} \right) + 4\text{Li}_2 \left( \frac{1 - \beta}{1 + \beta} \right) + \frac{1}{3}\pi^2 \right\} \right], \end{aligned} \quad (11)$$

$$\text{Re}B = \hat{\alpha}_s \frac{1 - \beta^2}{\beta} \log \frac{1 + \beta}{1 - \beta}, \quad (12)$$

$$\text{Im}B = -\hat{\alpha}_s\pi\frac{1-\beta^2}{\beta}, \quad (13)$$

where  $\hat{\alpha}_s = \alpha_s/(3\pi)$ ,  $\beta = \sqrt{1-4m_t^2/s}$ , and  $\text{Li}_2$  is the Spence function.  $\text{Re}A$  in eq. (11) contains the effective form factor for a cut-off  $\omega_{\text{max}}$  on the gluon energy after the infrared singularities have been cancelled between the virtual- and soft-gluon contributions in the on-shell renormalization scheme. Only the real part of the form factor  $A$  has been given, because the contribution of the imaginary part is proportional to the  $Z$  width, and hence negligibly small [15, 17]. The imaginary part of  $B$ , however, contributes to azimuthal distributions.

The helicity amplitudes for  $e^+e^- \rightarrow \gamma^*, Z^* \rightarrow t\bar{t}$  in the cm frame, including  $c_d^{\gamma,Z}$  and  $c_M^{\gamma,Z}$  couplings, have been given in [18] (see also Kane *et al.*, ref. [2]).

We write the contribution of a general  $tbW$  vertex to  $t$  and  $\bar{t}$  decays as

$$\begin{aligned} \Gamma_{tbW}^\mu = & -\frac{g}{\sqrt{2}}V_{tb}\bar{u}(p_b) \left[ \gamma^\mu(f_{1L}P_L + f_{1R}P_R) \right. \\ & \left. -\frac{i}{m_W}\sigma^{\mu\nu}(p_t - p_b)_\nu(f_{2L}P_L + f_{2R}P_R) \right] u(p_t), \end{aligned} \quad (14)$$

$$\begin{aligned} \bar{\Gamma}_{tbW}^\mu = & -\frac{g}{\sqrt{2}}V_{tb}^*\bar{v}(p_{\bar{t}}) \left[ \gamma^\mu(\bar{f}_{1L}P_L + \bar{f}_{1R}P_R) \right. \\ & \left. -\frac{i}{m_W}\sigma^{\mu\nu}(p_{\bar{t}} - p_{\bar{b}})_\nu(\bar{f}_{2L}P_L + \bar{f}_{2R}P_R) \right] v(p_{\bar{b}}), \end{aligned} \quad (15)$$

where  $P_{L,R} = \frac{1}{2}(1 \pm \gamma_5)$ , and  $V_{tb}$  is the Cabibbo-Kobayashi-Maskawa matrix element, which we take to be equal to one. If CP is conserved, the form factors  $f$  above obey the relations

$$f_{1L} = \bar{f}_{1L}; \quad f_{1R} = \bar{f}_{1R}, \quad (16)$$

and

$$f_{2L} = \bar{f}_{2R}; \quad f_{2R} = \bar{f}_{2L}. \quad (17)$$

Like  $c_d^\gamma$  and  $c_d^Z$  above, we will also treat  $f_{2L,R}$  and  $\bar{f}_{2L,R}$  as small, and retain only terms linear in them. For the form factors  $f_{1L}$  and  $\bar{f}_{1L}$ , we retain their SM values, viz.,  $f_{1L} = \bar{f}_{1L} = 1$ .  $f_{1R}$  and  $\bar{f}_{1R}$  do not contribute in the limit of vanishing  $b$  mass, which is used here. Also,  $f_{2L}$  and  $\bar{f}_{2R}$  drop out in this limit.

The helicity amplitudes for

$$t \rightarrow bW^+, \quad W^+ \rightarrow l^+\nu_l$$

and

$$\bar{t} \rightarrow \bar{b}W^-, \quad W^- \rightarrow l^-\bar{\nu}_l$$

in the respective rest frames of  $t, \bar{t}$ , in the limit that all masses except the top mass are neglected, are given in ref. [8].

Combining the production and decay amplitudes in the narrow-width approximation for  $t, \bar{t}, W^+, W^-$ , and using appropriate Lorentz boosts to calculate everything in the  $e^+e^-$  cm frame, we get the  $l^+$  and  $l^-$  angular distributions for the case of  $e^-, e^+$  with polarization  $P_e, P_{\bar{e}}$  to be:

$$\begin{aligned} \frac{d^3\sigma^\pm}{d\cos\theta_t d\cos\theta_l d\phi_l} &= \frac{3\alpha^2\beta m_t^2}{8s^2} B_t B_{\bar{t}} \frac{1}{(1 - \beta \cos\theta_{tl})^3} \\ &\times \left[ \mathcal{A}(1 - \beta \cos\theta_{tl}) + \mathcal{B}^\pm(\cos\theta_{tl} - \beta) \right. \\ &\quad + \mathcal{C}^\pm(1 - \beta^2) \sin\theta_t \sin\theta_l (\cos\theta_t \cos\phi_l - \sin\theta_t \cot\theta_l) \\ &\quad \left. + \mathcal{D}^\pm(1 - \beta^2) \sin\theta_t \sin\theta_l \sin\phi_l \right], \end{aligned} \quad (18)$$

where  $\sigma^+$  and  $\sigma^-$  refer respectively to  $l^+$  and  $l^-$  distributions, with the same notation for the kinematic variables of particles and antiparticles. Thus,  $\theta_t$ , is the polar angle of  $t$  (or  $\bar{t}$ ), and  $E_l, \theta_l, \phi_l$  are the energy, polar angle and azimuthal angle of  $l^+$  (or  $l^-$ ). All the angles are now in the cm frame, with the  $z$  axis chosen along the  $e^-$  momentum, and the  $x$  axis chosen in the plane containing the  $e^-$  and  $t$  directions.  $\theta_{tl}$  is the angle between the  $t$  and  $l^+$  directions (or  $\bar{t}$  and  $l^-$  directions).  $\beta$  is the  $t$  (or  $\bar{t}$ ) velocity:  $\beta = \sqrt{1 - 4m_t^2/s}$ , and  $\gamma = 1/\sqrt{1 - \beta^2}$ .  $B_t$  and  $B_{\bar{t}}$  are respectively the branching ratios of  $t$  and  $\bar{t}$  into the final states being considered.

The coefficients  $\mathcal{A}^\pm, \mathcal{B}^\pm, \mathcal{C}^\pm$  and  $\mathcal{D}^\pm$  are given by

$$\mathcal{A} = A_0 + A_1 \cos\theta_t + A_2 \cos^2\theta_t, \quad (19)$$

$$\mathcal{B}^\pm = B_0^\pm + B_1 \cos\theta_t + B_2^\pm \cos^2\theta_t, \quad (20)$$

$$\mathcal{C}^\pm = C_0^\pm + C_1^\pm \cos\theta_t, \quad (21)$$

$$\mathcal{D}^\pm = D_0^\pm + D_1^\pm \cos\theta_t, \quad (22)$$

The quantities  $A_i, B_i^\pm, C_i^\pm$  and  $D_i^\pm$  occurring in the above equation are functions of the masses,  $s$ , the degrees of  $e$  and  $\bar{e}$  polarization ( $P_e$  and  $P_{\bar{e}}$ ), and the coupling constants. They are listed in the Appendix.

It should be emphasized that, as shown in [7, 8], the distribution in (18) does not depend on anomalous effects in the  $tbW$  vertices (14) and (15). Thus even  $\mathcal{O}(\alpha_s)$  QCD corrections to the  $tbW$  vertices would not be felt in (18).

To obtain the single-differential polar-angle distribution, we integrate over  $\phi$  from 0 to  $2\pi$ , and finally over  $\cos \theta_l$  from  $-1$  to  $+1$ . The final result is

$$\begin{aligned}
\frac{d\sigma^\pm}{d\cos\theta_l} = & \frac{3\pi\alpha^2}{32s} B_t B_{\bar{t}} \beta \left\{ 4A_0 \mp 2A_1 \left( \frac{1-\beta^2}{\beta^2} \log \frac{1+\beta}{1-\beta} - \frac{2}{\beta} \right) \cos\theta_l \right. \\
& + 2A_2 \left( \frac{1-\beta^2}{\beta^3} \log \frac{1+\beta}{1-\beta} (1-3\cos^2\theta_l) \right. \\
& \left. \left. - \frac{2}{\beta^2} (1-3\cos^2\theta_l - \beta^2 + 2\beta^2 \cos^2\theta_l) \right) \right. \\
& \pm 2B_1 \frac{1-\beta^2}{\beta^2} \left( \frac{1}{\beta} \log \frac{1+\beta}{1-\beta} - 2 \right) \cos\theta_l \\
& + B_2^\pm \frac{1-\beta^2}{\beta^3} \left( \frac{\beta^2-3}{\beta} \log \frac{1+\beta}{1-\beta} + 6 \right) (1-3\cos^2\theta_l) \\
& \pm 2C_0^\pm \frac{1-\beta^2}{\beta^2} \left( \frac{1-\beta^2}{\beta} \log \frac{1+\beta}{1-\beta} - 2 \right) \cos\theta_l \\
& \left. - C_1^\pm \frac{1-\beta^2}{\beta^3} \left( \frac{3(1-\beta^2)}{\beta} \log \frac{1+\beta}{1-\beta} - 2(3-2\beta^2) \right) (1-3\cos^2\theta_l) \right\}. \quad (23)
\end{aligned}$$

This is the same expression as in [5] and [8]. However, the significance of the functions  $A_i$ ,  $B_i$ ,  $C_i$  and  $D_i$  is different in each case.

We now proceed to a discussion of  $CP$ -odd asymmetries resulting from the use of the above distributions.

### 3 $CP$ -violating angular asymmetries

We will work with two different types of asymmetries, one which does not depend on the azimuthal angles angle of the decay lepton, so that the azimuthal angle is fully integrated over, and the other dependent on the azimuthal angle. In all cases, we assume a cut-off of  $\theta_0$  on the forward and backward directions of the charged lepton. Some cut-off on the forward and backward angles is certainly needed from an experimental point of view; we furthermore exploit the cut-off to optimize the sensitivity.

In the first case, namely polar asymmetries, we define two independent  $CP$ -violating asymmetries, which depend on different linear combinations of  $\text{Im}c_d^\gamma$



and  $\text{Im}c_d^Z$ . (It is not possible to define  $CP$ -odd quantities which determine  $\text{Re}c_d^{\gamma,Z}$  using single-lepton polar distributions, as can be seen from the expression for the  $CP$ -odd combination  $\frac{d\sigma^+}{d\cos\theta_l}(\theta_l) - \frac{d\sigma^-}{d\cos\theta_l}(\pi - \theta_l)$ ). One is simply the total lepton-charge asymmetry, with a cut-off of  $\theta_0$  on the forward and backward directions:

$$A_{ch}(\theta_0) = \frac{\int_{\theta_0}^{\pi-\theta_0} d\theta_l \left( \frac{d\sigma^+}{d\theta_l} - \frac{d\sigma^-}{d\theta_l} \right)}{\int_{\theta_0}^{\pi-\theta_0} d\theta_l \left( \frac{d\sigma^+}{d\theta_l} + \frac{d\sigma^-}{d\theta_l} \right)}. \quad (24)$$

The other is the leptonic forward-backward asymmetry combined with charge asymmetry, again with the angles within  $\theta_0$  of the forward and backward directions excluded:

$$A_{fb}(\theta_0) = \frac{\int_{\theta_0}^{\frac{\pi}{2}} d\theta_l \left( \frac{d\sigma^+}{d\theta_l} + \frac{d\sigma^-}{d\theta_l} \right) - \int_{\frac{\pi}{2}}^{\pi-\theta_0} d\theta_l \left( \frac{d\sigma^+}{d\theta_l} + \frac{d\sigma^-}{d\theta_l} \right)}{\int_{\theta_0}^{\pi-\theta_0} d\theta_l \left( \frac{d\sigma^+}{d\theta_l} + \frac{d\sigma^-}{d\theta_l} \right)}. \quad (25)$$

Analytic expressions for both these asymmetries may be easily obtained using (23), and are not displayed here explicitly.

We note the fact that  $A_{ch}(\theta_0)$  vanishes for  $\theta_0 = 0$ . This implies that the  $CP$ -violating charge asymmetry does not exist unless a cut-off is imposed on the lepton production angle.  $A_{fb}(\theta_0)$ , however, is nonzero for  $\theta_0 = 0$ .

We now define angular asymmetries of the second type, which depend on the range of the azimuthal angle  $\phi_l$  of the charged lepton. These are called the up-down and left-right asymmetries, and depend respectively on the real and imaginary parts of the dipole couplings.

The up-down asymmetry [5] is defined by

$$A_{ud}(\theta_0) = \frac{1}{2\sigma(\theta_0)} \int_{\theta_0}^{\pi-\theta_0} \left[ \frac{d\sigma_{\text{up}}^+}{d\theta_l} - \frac{d\sigma_{\text{down}}^+}{d\theta_l} + \frac{d\sigma_{\text{up}}^-}{d\theta_l} - \frac{d\sigma_{\text{down}}^-}{d\theta_l} \right] d\theta_l, \quad (26)$$

where

$$\sigma(\theta_0) = \int_{\theta_0}^{\pi-\theta_0} \frac{d\sigma}{d\theta_l} d\theta_l \quad (27)$$

is the SM cross section for the semi-leptonic final state, with a forward and backward cut-off of  $\theta_0$  on  $\theta_l$ . Here up/down refers to  $(p_{l\pm})_y \gtrless 0$ ,  $(p_{l\pm})_y$  being

the  $y$  component of  $\vec{p}_{l\pm}$  with respect to a coordinate system chosen in the  $e^+e^-$  center-of-mass (cm) frame so that the  $z$ -axis is along  $\vec{p}_e$ , and the  $y$ -axis is along  $\vec{p}_e \times \vec{p}_t$ . The  $t\bar{t}$  production plane is thus the  $xz$  plane. Thus, “up” refers to the range  $0 < \phi_l < \pi$ , and “down” refers to the range  $\pi < \phi_l < 2\pi$ .

The left-right asymmetry is defined by

$$A_{lr}(\theta_0) = \frac{1}{2\sigma(\theta_0)} \int_{\theta_0}^{\pi-\theta_0} \left[ \frac{d\sigma_{\text{left}}^+}{d\theta_l} - \frac{d\sigma_{\text{right}}^+}{d\theta_l} + \frac{d\sigma_{\text{left}}^-}{d\theta_l} - \frac{d\sigma_{\text{right}}^-}{d\theta_l} \right] d\theta_l, \quad (28)$$

Here left/right refers to  $(p_{l\pm})_x \gtrless 0$ ,  $(p_{l\pm})_x$  being the  $x$  component of  $\vec{p}_{l\pm}$  with respect to the coordinate system defined above. Thus, “left” refers to the range  $-\pi/2 < \phi_l < \pi/2$ , and “right” refers to the range  $\pi/2 < \phi_l < 3\pi/2$ .

Analytic expressions for the up-down and left-right symmetry are not available for nonzero cut-off in  $\theta_l$ . Hence, the angular integrations have been done numerically in what follows.

Two other asymmetries were defined in [4], which helped to disentangle the two dipole couplings from each other. However, we do not discuss these here. Instead, we will assume that the electron beam polarization can be made to change sign to give additional observable quantities to enable this disentanglement.

All these asymmetries are a measure of  $CP$  violation in the unpolarized case and in the case when polarization is present, but  $P_e = -P_{\bar{e}}$ . When  $P_e \neq -P_{\bar{e}}$ , the initial state is not invariant under  $CP$ , and therefore  $CP$ -invariant interactions can contribute to the asymmetries. However, to leading order in  $\alpha$ , these  $CP$ -invariant contributions vanish in the limit  $m_e = 0$ . Order- $\alpha$  collinear helicity-flip photon emission can give a  $CP$ -even contribution. However, this background has been estimated in [19], and found to be negligible for certain  $CP$ -odd correlations for the kind of luminosities under consideration. It has also been estimated for  $A_{fb}$  and  $A_{ch}$ , and again found negligible [20]. The background is zero in the case of  $A_{ud}$  [20]. It is expected that the background will also be negligible for  $A_{lr}$  though it has not been calculated explicitly.

## 4 Numerical Results

In this section we describe the numerical results for the calculation of 90% confidence level (CL) limits that could be put on  $\text{Re}c_d^{\gamma,Z}$  and  $\text{Im}c_d^{\gamma,Z}$  using the asymmetries described in the previous sections.

We look at only semileptonic final states. That is to say, when  $t$  decays leptonically, we assume  $\bar{t}$  decays hadronically, and *vice versa*. We sum over the electron and muon decay channels. Thus,  $B_t B_{\bar{t}}$  is taken to be  $2/3 \times 2/9$ .

We have considered unpolarized beams, as well as the case when the electron beam has a longitudinal polarization of 90%, either left-handed or right-handed. We have also considered the possibility of two runs for identical time-spans with the polarization reversed in the second run. The positron beam is assumed to be unpolarized.

We assume an integrated luminosity of  $200 \text{ fb}^{-1}$  for a cm energy of 500 GeV, and an integrated luminosity of  $1000 \text{ fb}^{-1}$  for a cm energy of 1000 GeV. The limits for higher luminosities can easily be obtained by scaling down the limits presented here by the square root of the factor by which the luminosity is scaled up.

We use the parameters  $\alpha = 1/128$ ,  $\alpha_s(m_Z^2) = 0.118$ ,  $m_Z = 91.187 \text{ GeV}$ ,  $m_W = 80.41 \text{ GeV}$ ,  $m_t = 175 \text{ GeV}$  and  $\sin^2 \theta_W = 0.2315$ . We have used, following [15], a gluon energy cut-off of  $\omega_{\max} = (\sqrt{s} - 2m_t)/5$ . While qualitative results would be insensitive, exact quantitative results would of course depend on the choice of cut-off.

Fig. 1 shows the SM cross section  $\sigma(\theta_0)$ , defined in eq. (27), for  $t$  or  $\bar{t}$  production, followed by its semileptonic decay, with a cut-off  $\theta_0$  on the lepton polar angle, plotted against  $\theta_0$  for the two choices of  $\sqrt{s}$  and for different electron beam polarizations.

Tables 1-5 show the results on the limits obtainable for each of these possibilities. In all cases, the value of the cut-off  $\theta_0$  has been chosen to get the best sensitivity for that specific item.

In Table 1 we give the 90% confidence level (CL) limits that can be obtained on  $\text{Im}c_d^\gamma$  and  $\text{Im}c_d^Z$ , assuming one of them to be nonzero, the other taken to be vanishing. The limit is defined as the value of  $\text{Im}c_d^\gamma$  or  $\text{Im}c_d^Z$  for which the corresponding asymmetry  $A_{ch}$  or  $A_{fb}$  becomes equal to  $1.64/\sqrt{N}$ , where  $N$  is the total number of events.

Table 2 shows possible 90% CL limits for the unpolarized case, when results from  $A_{ch}$  and  $A_{fb}$  are combined. The idea is that each asymmetry measures a different linear combination of  $\text{Im}c_d^\gamma$  and  $\text{Im}c_d^Z$ . So a null result for the two asymmetries will correspond to two different bands of regions allowed at 90% CL in the space of  $\text{Im}c_d^\gamma$  and  $\text{Im}c_d^Z$ . The overlapping region of the two bands leads to the limits given in Table 2. In this case, for 90% CL, the asymmetry is required to be  $2.15/\sqrt{N}$ , corresponding to two degrees of freedom. Incidentally, the same

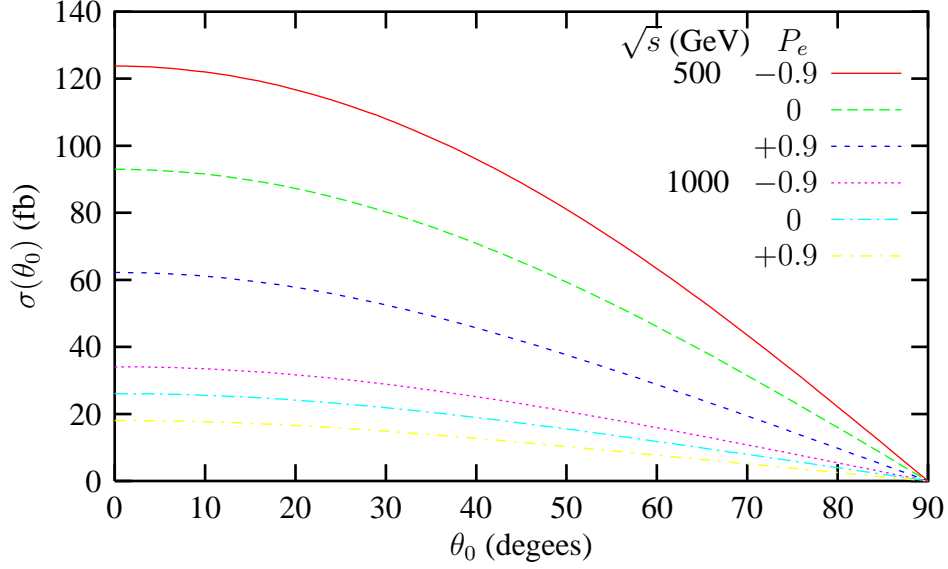


Figure 1: The SM cross section for decay leptons in the process  $e^+e^- \rightarrow t\bar{t}$  plotted as a function of the cut-off  $\theta_0$  on the lepton polar angle in the forward and backward directions for  $e^-$  beam longitudinal polarizations  $P_e = -0.9, 0, +0.9$  and for values of total cm energy  $\sqrt{s} = 500$  GeV and  $\sqrt{s} = 1000$  GeV.

$\sqrt{s}$ (GeV)	$P_e$	$A_{ch}$			$A_{fb}$		
		$\theta_0$	$\text{Im}c_d^\gamma$	$\text{Im}c_d^Z$	$\theta_0$	$\text{Im}c_d^\gamma$	$\text{Im}c_d^Z$
500	0	$64^\circ$	0.084	0.49	$10^\circ$	0.086	0.95
	+0.9	$64^\circ$	0.081	0.17	$10^\circ$	0.075	0.15
	-0.9	$64^\circ$	0.083	0.14	$10^\circ$	0.093	0.15
1000	0	$64^\circ$	0.029	0.18	$10^\circ$	0.032	0.36
	+0.9	$64^\circ$	0.028	0.061	$10^\circ$	0.028	0.058
	-0.9	$64^\circ$	0.028	0.047	$10^\circ$	0.034	0.058

Table 1: Individual 90% CL limits on dipole couplings obtainable from  $A_{ch}$  and  $A_{fb}$  for  $\sqrt{s} = 500$  GeV with integrated luminosity  $200 \text{ fb}^{-1}$  and for  $\sqrt{s} = 1000$  GeV with integrated luminosity  $1000 \text{ fb}^{-1}$  for different electron beam polarizations  $P_e$ . Cut-off  $\theta_0$  is chosen to optimize the sensitivity.

$\sqrt{s}$ (GeV)	$\theta_0$	$\text{Im}c_d^\gamma$	$\text{Im}c_d^Z$
500	40°	0.53	4.1
1000	40°	0.20	1.5

Table 2: Simultaneous 90% CL limits on dipole couplings obtainable from  $A_{ch}$  and  $A_{fb}$  for  $\sqrt{s} = 500$  GeV with integrated luminosity  $200 \text{ fb}^{-1}$  and for  $\sqrt{s} = 1000$  GeV with integrated luminosity  $1000 \text{ fb}^{-1}$  for unpolarized beams. Cut-off  $\theta_0$  is chosen to optimize the sensitivity.

$\sqrt{s}$ (GeV)	$A_{ch}$			$A_{fb}$		
	$\theta_0$	$\text{Im}c_d^\gamma$	$\text{Im}c_d^Z$	$\theta_0$	$\text{Im}c_d^\gamma$	$\text{Im}c_d^Z$
500	64°	0.11	0.20	10°	0.11	0.20
1000	64°	0.037	0.069	10°	0.040	0.076

Table 3: Simultaneous limits on dipole couplings combining data from polarizations  $P_e = 0.9$  and  $P_e = -0.9$ , using separately  $A_{ch}$  and  $A_{fb}$  for  $\sqrt{s} = 500$  GeV with integrated luminosity  $200 \text{ fb}^{-1}$  and for  $\sqrt{s} = 1000$  GeV with integrated luminosity  $1000 \text{ fb}^{-1}$ . Cut-off  $\theta_0$  is chosen to optimize the sensitivity.

procedure followed for  $P_e = \pm 0.9$  gives much worse limits.

Similarly, using one of the two asymmetries, but two different polarizations of the electron beam, one can get two bands in the parameter plane, which give simultaneous limits on the dipole couplings. The results for electron polarizations  $P_e = \pm 0.9$  are given in Table 3 for each of the asymmetries  $A_{ch}$  and  $A_{fb}$ .

Table 4 lists the 90% CL limits which may be obtained on the real and imaginary parts of the dipole couplings using  $A_{ud}$  and  $A_{lr}$ , assuming one of the couplings to be nonzero at a time.

Table 5 shows simultaneous limits on  $\text{Re}c_d^\gamma$  and  $\text{Re}c_d^Z$  obtainable from combining the data on  $A_{ud}$  for  $P_e = +0.9$  and  $P_e = -0.9$ , and similarly, limits on  $\text{Im}c_d^\gamma$  and  $\text{Im}c_d^Z$  from data on  $A_{lr}$  for the two polarizations.

$\sqrt{s}$ (GeV)	$P_e$	$A_{ud}$			$A_{lr}$		
		$\theta_0$	$\text{Rec}_d^\gamma$	$\text{Rec}_d^Z$	$\theta_0$	$\text{Im}c_d^\gamma$	$\text{Im}c_d^Z$
500	0	25°	0.10	0.034	30°	0.024	0.14
	+0.9	30°	0.025	0.037	35°	0.024	0.050
	-0.9	25°	0.022	0.032	30°	0.023	0.038
1000	0	30°	0.029	0.0096	60°	0.021	0.13
	+0.9	35°	0.0068	0.010	60°	0.021	0.045
	-0.9	30°	0.0061	0.0089	60°	0.021	0.035

Table 4: Individual 90% CL limits on dipole couplings obtainable from  $A_{ud}$  and  $A_{lr}$  for  $\sqrt{s} = 500$  GeV with integrated luminosity  $200 \text{ fb}^{-1}$  and for  $\sqrt{s} = 1000$  GeV with integrated luminosity  $1000 \text{ fb}^{-1}$  for different electron beam polarizations  $P_e$ . Cut-off  $\theta_0$  is chosen to optimize the sensitivity.

$\sqrt{s}$ (GeV)	$A_{ud}$			$A_{lr}$		
	$\theta_0$	$\text{Rec}_d^\gamma$	$\text{Rec}_d^Z$	$\theta_0$	$\text{Im}c_d^\gamma$	$\text{Im}c_d^Z$
500	25°	0.031	0.045	35°	0.031	0.056
1000	30°	0.0085	0.013	60°	0.028	0.052

Table 5: Simultaneous limits on dipole couplings combining data from polarizations  $P_e = 0.9$  and  $P_e = -0.9$ , using separately  $A_{ud}$  and  $A_{lr}$  for  $\sqrt{s} = 500$  GeV with integrated luminosity  $200 \text{ fb}^{-1}$  and for  $\sqrt{s} = 1000$  GeV with integrated luminosity  $1000 \text{ fb}^{-1}$ . Cut-off  $\theta_0$  is chosen to optimize the sensitivity.

## 5 Conclusions

We have presented in analytic form the single-lepton angular distribution in the production and subsequent decay of  $t\bar{t}$  in the presence of electric and weak dipole form factors of the top quark. We have included  $\mathcal{O}(\alpha_s)$  QCD corrections in SGA. Anomalous contributions to the  $tbW$  decay vertex do not affect these distributions. We have also included effects of longitudinal electron beam polarization of 90%, while assuming the positron beam to be unpolarized. We have then obtained analytic expressions for certain simple  $CP$ -violating polar-angle asymmetries, specially chosen so that they do not require the reconstruction of the  $t$  or  $\bar{t}$  directions or energies. We have also evaluated numerically azimuthal asymmetries which need minimal information on the  $t$  or  $\bar{t}$  momentum direction alone. We have analyzed these asymmetries to obtain simultaneous 90% CL limits on the electric and weak dipole couplings which would be possible at future linear  $e^+e^-$  collider like the proposed JLC operating at  $\sqrt{s} = 500$  GeV with an integrated luminosity of  $200 \text{ fb}^{-1}$ , and at  $\sqrt{s} = 1000$  GeV with an integrated luminosity of  $1000 \text{ fb}^{-1}$ .

In general, simultaneous 90% CL limits on  $c_d^\gamma$  and  $c_d^Z$  which can be obtained with the polarized 500 GeV option are of the order of 0.1–0.2, corresponding to dipole moments of about  $(1 - 2) \times 10^{-17} e \text{ cm}$ , if the asymmetries  $A_{ch}$  or  $A_{fb}$  are used. The limits improve by a factor of 3 or 4 if the azimuthal asymmetries  $A_{ud}$  or  $A_{lr}$  are used. However, putting in a top detection efficiency factor of 10% in the case of azimuthal asymmetries, where top direction needs to be determined, would bring down these limits to the same level of  $(1 - 2) \times 10^{-17} e \text{ cm}$ .

For  $\sqrt{s} = 1000$  GeV and an integrated luminosity of  $1000 \text{ fb}^{-1}$ , the limits obtainable would be better by a factor of 3 or 4 in each case, bringing them to the level of  $(2 - 3) \times 10^{-18} e \text{ cm}$  in the best cases.

Our general conclusion is that the sensitivity to the measurement of individual dipole couplings  $\text{Re}c_d^\gamma$  and  $\text{Im}c_d^Z$  is improved considerably if the electron beam is polarized, a situation which might easily obtain at linear colliders. As a consequence, simultaneous limits on all the couplings are improved by beam polarization.

The theoretical predictions for  $c_d^{\gamma,Z}$  are at the level of  $10^{-2} - 10^{-3}$ , as for example, in the neutral-Higgs-exchange and supersymmetric models of CP violation [9, 18, 21, 3]. In other models, like the charged-Higgs-exchange [3] or third-generation leptoquark models [22], the prediction are even lower. Hence the measurements suggested here at the 500 GeV option cannot exclude these modes at the 90% C.L. It will be necessary to use the 1000 GeV option with a suitable

luminosity to test at least some of the models.

It is necessary to repeat this study including experimental detection efficiencies. Given an overall efficiency, we could still get an idea of the limits on the dipole couplings by scaling them as the inverse square root of the efficiency.

We have not included a cut-off on decay-lepton energies which may be required from a practical point of view. However, our results are perfectly valid if the cut-off is reasonably small. For example, for  $\sqrt{s} = 500$  GeV, the minimum lepton energy allowed kinematically is about 7.5 GeV. So a cut-off below that would need no modification of the results.

We have restricted ourselves to energies in the  $t\bar{t}$  continuum. Studies in the threshold region are also interesting and have been investigated in [23].

## Appendix

The expressions for  $A_i$ ,  $B_i$ ,  $C_i$  and  $D_i$  occurring in equation (8) are listed below. They include to first order the form factors  $c_d^\gamma$  and  $c_d^Z$ , as well as  $c_M^\gamma$  and  $c_M^Z$ . Terms containing products of  $c_d^{\gamma,Z}$  with  $c_M^{\gamma,Z}$  have been dropped. It is also understood that terms proportional to products of  $A$  or  $B$  (which are of order  $\alpha_s$ ) and  $c_d^\gamma$  or  $c_d^Z$  have to be omitted in the calculations.

$$\begin{aligned}
A_0 &= 2 \left\{ (2 - \beta^2) \left[ 2|c_v^\gamma|^2 + 2(r_L + r_R)\text{Re}(c_v^\gamma c_v^{Z*}) + (r_L^2 + r_R^2)|c_v^Z|^2 \right] \right. \\
&\quad + \beta^2(r_L^2 + r_R^2)|c_a^Z|^2 - 2\beta^2 [2\text{Re}(c_v^\gamma c_M^{\gamma*}) \\
&\quad + (r_L + r_R)\text{Re}(c_v^\gamma c_M^{Z*} + c_v^Z c_M^{\gamma*}) + (r_L^2 + r_R^2)\text{Re}(c_v^Z c_M^{Z*})] (1 - P_e P_{\bar{e}}) \\
&\quad + (2 - \beta^2) \left[ 2(r_L - r_R)\text{Re}(c_v^\gamma c_v^{Z*}) + (r_L^2 - r_R^2)|c_v^Z|^2 \right] \\
&\quad + \beta^2(r_L^2 - r_R^2)|c_a^Z|^2 - 2\beta^2 [(r_L - r_R)\text{Re}(c_v^\gamma c_M^{Z*} + c_v^Z c_M^{\gamma*}) \\
&\quad + (r_L^2 - r_R^2)\text{Re}(c_v^Z c_M^{Z*})] \left. \right\} (P_{\bar{e}} - P_e), \\
A_1 &= -8\beta\text{Re} \left( c_a^{Z*} \left\{ [(r_L - r_R)c_v^\gamma + (r_L^2 - r_R^2)c_v^Z] (1 - P_e P_{\bar{e}}) \right. \right. \\
&\quad \left. \left. + [(r_L + r_R)c_v^\gamma + (r_L^2 + r_R^2)c_v^Z] (P_{\bar{e}} - P_e) \right\} \right), \\
A_2 &= 2\beta^2 \left\{ [2|c_v^\gamma|^2 + 4\text{Re}(c_v^\gamma c_M^{\gamma*}) + 2(r_L + r_R)\text{Re}(c_v^\gamma c_v^{Z*} + c_v^Z c_M^{\gamma*} + c_v^Z c_M^{\gamma*})] \right.
\end{aligned}$$



$$\begin{aligned}
& + (r_L^2 + r_R^2) \left( |c_v^Z|^2 + |c_a^Z|^2 + 2\text{Re}(c_v^Z c_M^{Z*}) \right) \left( 1 - P_e P_{\bar{e}} \right) \\
& + \left[ 2(r_L - r_R) \text{Re}(c_v^\gamma c_v^{Z*} + c_v^\gamma c_M^{Z*} + c_v^Z c_M^{\gamma*}) \right. \\
& \left. + (r_L^2 - r_R^2) \left( |c_v^Z|^2 + |c_a^Z|^2 + 2\text{Re}(c_v^Z c_M^{Z*}) \right) \right] (P_{\bar{e}} - P_e) \Big\}, \\
B_0^\pm &= 4\beta \left\{ \left( \text{Rec}_v^\gamma + r_L \text{Rec}_v^Z \right) \left( r_L \text{Rec}_a^Z \mp \text{Im}c_d^\gamma \mp r_L \text{Im}c_d^Z \right) (1 - P_e)(1 + P_{\bar{e}}) \right. \\
& \left. + \left( \text{Rec}_v^\gamma + r_R \text{Rec}_v^Z \right) \left( r_R \text{Rec}_a^Z \mp \text{Im}c_d^\gamma \mp r_R \text{Im}c_d^Z \right) (1 + P_e)(1 - P_{\bar{e}}) \right\}, \\
B_1 &= -4 \left\{ \left[ |c_v^\gamma + r_L c_v^Z|^2 + \beta^2 r_L^2 |c_a^Z|^2 \right] (1 - P_e)(1 + P_{\bar{e}}) \right. \\
& \left. - \left[ |c_v^\gamma + r_R c_v^Z|^2 + \beta^2 r_R^2 |c_a^Z|^2 \right] (1 + P_e)(1 - P_{\bar{e}}) \right\}, \\
B_2^\pm &= 4\beta \left\{ \left( \text{Rec}_v^\gamma + r_L \text{Rec}_v^Z \right) \left( r_L \text{Rec}_a^Z \pm \text{Im}c_d^\gamma \pm r_L \text{Im}c_d^Z \right) (1 - P_e)(1 + P_{\bar{e}}) \right. \\
& \left. + \left( \text{Rec}_v^\gamma + r_R \text{Rec}_v^Z \right) \left( r_R \text{Rec}_a^Z \pm \text{Im}c_d^\gamma \pm r_R \text{Im}c_d^Z \right) (1 + P_e)(1 - P_{\bar{e}}) \right\}, \\
C_0^\pm &= 4 \left\{ \left[ |c_v^\gamma + r_L c_v^Z|^2 - \beta^2 \gamma^2 \left( \text{Rec}_v^\gamma + r_L \text{Rec}_v^Z \right) \left( \text{Rec}_M^\gamma + r_L \text{Rec}_M^Z \right) \right. \right. \\
& \left. \pm \beta^2 \gamma^2 r_L \text{Rec}_a^Z \left( \text{Im}c_d^\gamma + \text{Im}c_d^Z r_L \right) \right] (1 - P_e)(1 + P_{\bar{e}}) \\
& \left. - \left[ |c_v^\gamma + r_R c_v^Z|^2 - \beta^2 \gamma^2 \left( \text{Rec}_v^\gamma + r_R \text{Rec}_v^Z \right) \left( \text{Rec}_M^\gamma + r_R \text{Rec}_M^Z \right) \right. \right. \\
& \left. \left. \pm \beta^2 \gamma^2 r_R \text{Rec}_a^Z \left( \text{Im}c_d^\gamma + \text{Im}c_d^Z r_R \right) \right] (1 + P_e)(1 - P_{\bar{e}}) \right\}, \\
C_1^\pm &= -4\beta \left\{ \left[ \left( \text{Rec}_v^\gamma + r_L \text{Rec}_v^Z \right) \left( r_L \text{Rec}_a^Z \pm \gamma^2 \text{Im}c_d^\gamma \pm r_L \gamma^2 \text{Im}c_d^Z \right) \right. \right. \\
& \left. - \beta^2 \gamma^2 r_L \text{Rec}_a^Z \left( \text{Rec}_M^\gamma + r_L \text{Rec}_M^Z \right) \right] (1 - P_e)(1 + P_{\bar{e}}) \\
& \left. + \left[ \left( \text{Rec}_v^\gamma + r_R \text{Rec}_v^Z \right) \left( r_R \text{Rec}_a^Z \pm \gamma^2 \text{Im}c_d^\gamma \pm r_R \gamma^2 \text{Im}c_d^Z \right) \right. \right. \\
& \left. - \beta^2 \gamma^2 r_R \text{Rec}_a^Z \left( \text{Rec}_M^\gamma + r_R \text{Rec}_M^Z \right) \right] (1 + P_e)(1 - P_{\bar{e}}) \right\}, \\
D_0^\pm &= 4\beta \left\{ \left[ \text{Im} \left[ \left( (c_v^\gamma + r_L c_v^Z) - \beta^2 \gamma^2 (c_M^\gamma + r_L c_M^Z) \right) r_L c_a^{Z*} \right] \right. \right. \\
& \left. \mp \gamma^2 \left( \text{Rec}_v^\gamma + r_L \text{Rec}_v^Z \right) \left( \text{Rec}_d^\gamma + r_L \text{Rec}_d^Z \right) \right] (1 - P_e)(1 + P_{\bar{e}}) \\
& \left. - \left[ \text{Im} \left[ \left( (c_v^\gamma + r_R c_v^Z) - \beta^2 \gamma^2 (c_M^\gamma + r_R c_M^Z) \right) r_R c_a^{Z*} \right] \right. \right. \\
& \left. \mp \gamma^2 \left( \text{Rec}_v^\gamma + r_R \text{Rec}_v^Z \right) \left( \text{Rec}_d^\gamma + r_R \text{Rec}_d^Z \right) \right] (1 + P_e)(1 - P_{\bar{e}}) \right\}, \\
D_1^\pm &= 4\beta^2 \gamma^2 \left\{ \left[ \left( \text{Rec}_v^\gamma + r_L \text{Rec}_v^Z \right) (\text{Im}c_M^\gamma \right. \right. \\
& \left. \left. + r_L \text{Im}c_M^Z) \pm r_L \text{Rec}_a^Z \left( \text{Rec}_d^\gamma + r_L \text{Rec}_d^Z \right) \right] (1 - P_e)(1 + P_{\bar{e}}) \right. \\
& \left. + \left[ \left( \text{Rec}_v^\gamma + r_R \text{Rec}_v^Z \right) (\text{Im}c_M^\gamma + r_R \text{Im}c_M^Z) \right. \right.
\end{aligned}$$

$$\pm r_R \text{Rec}_a^Z \left( \text{Rec}_d^\gamma + r_R \text{Rec}_d^Z \right) \left( 1 + P_e \right) \left( 1 - P_{\bar{e}} \right) \}.$$

Use has been made of

$$r_L = \frac{\left( \frac{1}{2} - x_W \right)}{(1 - m_Z^2/s) \sqrt{x_w(1 - x_w)}}$$

and

$$r_R = \frac{-x_W}{(1 - m_Z^2/s) \sqrt{x_w(1 - x_w)}}$$

in writing the above equation.

## References

- [1] I. Bigi and H. Krasemann, Z. Phys. C 7 (1981) 127; J. Kühn, Acta Phys. Austr. Suppl. XXIV (1982) 203; I. Bigi *et al.*, Phys. Lett. B 181 (1986) 157.
- [2] J.F. Donoghue and G. Valencia, Phys. Rev. Lett. 58 (1987) 451; C.A. Nelson, Phys. Rev. D 41 (1990) 2805; G.L. Kane, G.A. Ladinsky and C.-P. Yuan, Phys. Rev. D 45 (1991) 124; C.R. Schmidt and M.E. Peskin, Phys. Rev. Lett. 69 (1992) 410; C.R. Schmidt, Phys. Lett. B 293 (1992) 111; T. Arens and L.M. Sehgal, Phys. Rev. D 50 (1994) 4372.
- [3] D. Atwood, S. Bar-Shalom, G. Eilam and A. Soni, hep-ph/0006032.
- [4] P. Poulose and S.D. Rindani, Phys. Lett. B 349 (1995) 379.
- [5] P. Poulose and S.D. Rindani, Phys. Rev. D 54 (1996) 4326; 61 (2000) 119901 (E).
- [6] P. Poulose and S.D. Rindani, Phys. Lett. B 383 (1996) 212.
- [7] B. Grzadkowski and Z. Hioki, Phys. Lett. B 476 (2000) 87; hep-ph/0003294; Nucl. Phys. B 585 (2000) 3; Z. Hioki, hep-ph/0104105.
- [8] S.D. Rindani, Pramana J. Phys. 54 (2000) 791.

- [9] W. Bernreuther, T. Schröder and T.N. Pham, Phys. Lett. B 279 (1992) 389; W. Bernreuther and P. Overmann, Nucl. Phys. B 388 (1992) 53; Z. Phys. C 61 (1994) 599; W. Bernreuther and A. Brandenburg, Phys. Lett. B 314 (1993) 104; Phys. Rev. D 49 (1994) 4481; J.P. Ma and A. Brandenburg, Z. Phys. C 56 (1992) 97; A. Brandenburg and J.P. Ma, Phys. Lett. B 298 (1993) 211.
- [10] F. Cuypers and S.D. Rindani, Phys. Lett. B 343 (1994) 333.
- [11] D. Atwood and A. Soni, Phys. Rev. D 45 (1992) 2405; A. Bartl, E. Christova, T. Gajdosik and W. Majerotto, Phys. Rev. D 59 (1999) 077503.
- [12] S.M. Lietti and H. Murayama, Phys. Rev. D 62 (2000) 074003.
- [13] T. Arens and L.M. Sehgal, Nucl. Phys. B 393 (1993) 46.
- [14] S.D. Rindani, Phys. Lett. B 503 (2001) 292.
- [15] J. Kodaira, T. Nasuno and S. Parke, Phys. Rev. D 59 (1999) 014023.
- [16] M.M. Tung, J. Bernabéu and J. Peñarrocha, Nucl. Phys. B 470 (1996) 41; Phys. Lett. B 41 (198) 181.
- [17] V. Ravindran and W.L. van Nerven, Phys. Lett. B 445 (1998) 214; Phys. Lett. B 445 (1998) 206; Nucl. Phys. B 589 (2000) 507.
- [18] D. Chang, W.-Y. Keung and I. Phillips, Nucl. Phys. B 408 (1993) 286; 429 (1994) 255 (E).
- [19] B. Ananthanarayan and S.D. Rindani, Phys. Rev. D 52, (1995) 2684.
- [20] P. Poullose, Ph.D. thesis (1997) submitted to Gujarat University (unpublished).
- [21] A. Bartl, E. Christova and W. Majerotto, Nucl. Phys. B 460 (1996) 235; 465 (1996) 365 (E).
- [22] P. Poullose and S.D. Rindani, Pramana J. Phys. 51 (1998) 387.
- [23] M. Jezabek, T. Nagano and Y. Sumino, Phys. Rev. D 62 (2000) 014034; Y. Sumino, hep-ph/0007326.